SCIENTIFIC REP😊RTS

High Q-factor microring resonator wrapped by the curved waveguide

Dong-Po Cai[1], Jyun-Hong Lu[1], Chii-Chang Chen[1], Chien-Chieh Lee[2], Chu-En Lin[3] & Ta-Jen Yen[3]

In this work, we study the performances of ring resonators of different type by analyzing the bending loss and the condition of the critical coupling. We propose that the bending loss of microring can be reduced by wrapping a concentrically curved waveguide. The difference of propagation constant between two concentrically curved waveguides can be tuned by adjusting the bus waveguide width to optimize the critical coupling. Furthermore, we propose to enlarge the difference of the propagation constant between two concentrically curved waveguides to maintain the circulating light in the ring to obtain higher quality factor. In this study, the highest quality factor that we measured is 7×10^5.

The microring is an important and versatile integrated optics component. Several devices such as filter[1], gyroscope[2,3] and optical switch[4] can be constructed by the microring. Besides, the microring can provide the ultra-high Q-factor to induce the "slow light" property to slow down the group velocity of propagating light[5,6] and to improve the performance of gyroscope[2,3]. Over the past decade, several types of microring have been developed such as the single microring with single bus waveguide[7,8] or with double bus waveguides[9], the racetrack microring resonators[10] and the multiple microrings[11]. The results reported in Ref. 2 and Ref. 3 show that the improvement of the Q-factor of microring can enhance the sensitivity of gyroscope. The microdisk and microring with the pulley-type coupling configuration have been reported for the applications of integrated optical isolators[12,13] and sensor devices[14]. Recently, Cai *et al.* had reported the method to determine the coupling length and the propagation constant of the concentric waveguides[15]. This method is helpful to analyze the pulley-type microring.

In order to improve the Q-factor of microring, the maintenance of the light in the ring as long as possible (i.e, the reduction of the loss) is required due to the fact that Q-factor is inversely proportional to the decay constant of microring. Besides, the bending loss is one of the factors to mainly determine the performance of device for a microring structure. In the literatures, several guidelines in design, and cares during fabrication have been reported. For example, the sidewall roughness of the waveguides should be smoothed to decrease the scattering loss of waveguide[16,17]. For the racetrack microring, the increasing of the crosstalk between drop signal and add signal is critical[18]. The Q-factor can also be improved by increasing the radius of the microring to reduce the bending loss of the ring. By using the complex structure such as the multiple microrings[11], the performance of microring resonator can also be improved.

In this work, we propose a design guideline to improve the performance of microring. Firstly, by wrapping the bus waveguide around the curved part of the microring, the bending loss of microring can be reduced. A longer curved bus waveguide to wrap the microring may provide higher Q-factor. Secondly, the large difference of propagation constant between the bus waveguide and microring, $\Delta\beta$, (i.e. to reduce the light in the microring to couple toward the bus waveguide) is helpful to maintain the light in the ring. However, the condition of the critical coupling depends on $\Delta\beta$[19,20], and the increasing of $\Delta\beta$ should be finely tuned to optimize the critical coupling to improve the performance of microrings.

Several parameters of device including the ring waveguide width, bus waveguide width, radius of the ring and the gap width can be adjusted to enlarge $\Delta\beta$. To facilitate the analyses between the different

[1]Department of Optics and Photonics, National Central University, 32001 Jhongli, Taiwan. [2]Optical Sciences Center, National Central University, 32001 Jhongli, Taiwan. [3]Department of Materials Science and Engineering, National Tsing Hua University, Hsinchu 30013, Taiwan. Correspondence and requests for materials should be addressed to C.C.C. (email: trich@dop.ncu.edu.tw)
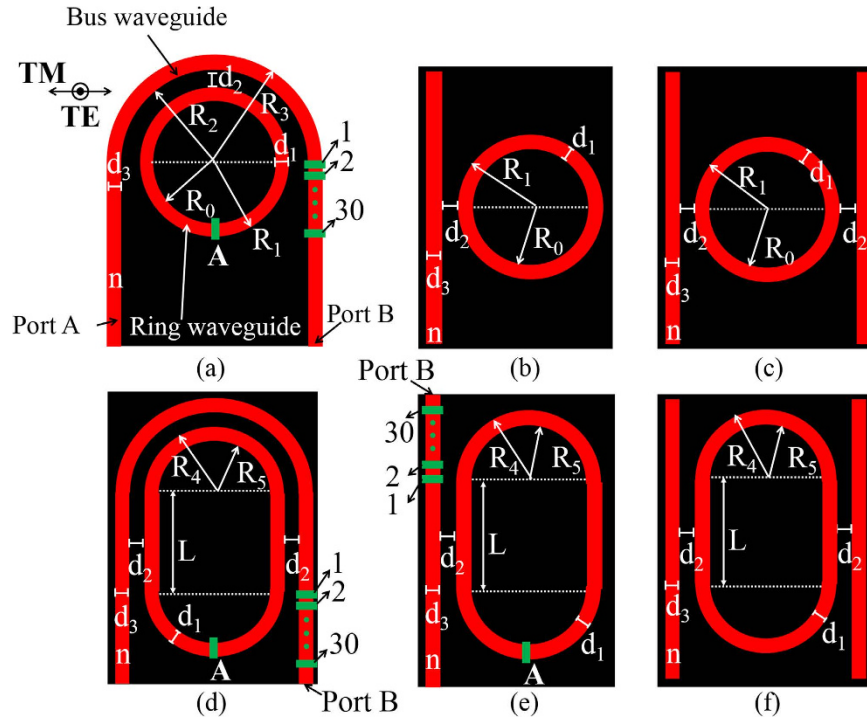
Figure 1. Schematic drawing of microring resonators. (**a**) shows pulley-type microring. (**b**) and (**c**) show microring with one bus waveguide and two bus waveguides, respectively. (**d**) shows pulley-type racetrack microring. (**e**) and (**f**) show racetrack microring with single bus waveguide and two bus waveguides, respectively. The green rectangles are the detectors to monitor the optical power.

types of microring, we fix the circumference of the ring, the ring waveguide width and the gap width. The width of the bus waveguides is adjusted to reach the critical coupling condition.

Results and Discussion

The various microring resonators. The various microrings and the parameters are schematically shown in Fig. 1(a)-(f). Fig. 1(a) is a pulley-type microring. Fig. 1(b),(c) are microrings with straight bus waveguide. Fig. 1 (d),(e),(f) are racetrack microrings. In Fig. 1(a)-(f), the circumference of the microrings is 27.835 μm for all cases. The inner radius, R_0, and the outer radius, R_1, of the microring are 4.33 μm and 4.53 μm in Fig. 1(a)-(c), respectively. For Fig. 1(a), the inner radius of the curved bus waveguide, R_2, is 4.68 μm. The outer radius of the curved bus waveguide, R_3, is varied from 4.83 μm to 4.93 μm. The corresponding width of the bus waveguide, d_3, is varied from 0.15 μm to 0.25 μm. For Fig. 1(d)-(f), the circumference of the racetrack microring is defined as $2L + 2\pi[(R_4 + R_5)/2]$ to be 27.835 μm where L, R_4 and R_5 are the length of the straight waveguide, the outer and inner radii of the curved waveguide in the racetrack, respectively. Moreover, L is varied from 0.5 π μm to 2.5 π μm. For all cases (Fig. 1(a)-(f)), the width of the ring waveguide, d_1, is 0.2 μm and the gap, d_2, between the ring waveguide and the bus waveguide is chosen to be 0.15 μm. The refractive index of the silicon waveguide for the wavelength range from 1 μm to 2 μm is obtained from Ref. 21 to be around 3.48 and the refractive index of the background is unity. The index contrast, $\Delta = (n_1^2 - n_2^2)/(2n_1^2)$, for different wavelengths is around 0.46 where n_1 is the index of waveguide and n_2 is the index of cladding layer. The absorption of the material is neglected in this work.

In 2-D finite-difference time-domain method (FDTD) simulation, a monitor is positioned in the ring. A pulse light source at the central wavelength of 1.55 μm with TM polarization is launched to obtain the spectrum of the light stored in the ring. The corresponding bandwidth of pulse is around 400 nm. The TM polarization is defined as the direction of electric field is perpendicular to the top surface of device. In order to estimate the Q-factor, the impulse light at the resonance wavelength is launched into the structure.

The Q-factors and the corresponding parameters for each microring resonator. For each resonator illustrated in Fig. 1, the difference of the propagation constant ($\Delta\beta$) is changed by varying d_3. We adopt the conformal transformation method[15,22,23] and Helmholtz equation to calculate the propagation constants of the waveguides. From Ref. 15, we concluded that the propagation constant of the outer curved waveguide is higher than that of the inner curved waveguide as the waveguide width is identical

Structure	Q-factor	d3 (μm)	L (μm)	λ (μm)	Index at resonant wavelength	Δβ	Corresponding field
Fig. 1(a)	7×10^5	0.23		1.49759	3.4808	3.4372	Fig. 2(a)
	1.4×10^3	0.15		1.499	3.4807	1.2103	Fig. 2(b)
Fig. 1(b)	1.24×10^5	0.25		1.00927	3.5878	10.2	Fig. 2(c)
	1.98×10^4	0.15		1.00928	3.5878	5.367	Fig. 2(d)
Fig. 1(c)	7.16×10^4	0.25		1.00927	3.5878	10.2	Fig. 2(e)
	9.06×10^3	0.15		1.00928	3.5878	5.367	Fig. 2(f)
Fig. 1(d)	3.6×10^4	0.20	2.5π	1.19055	3.521	4.465* / 0**	Fig. 2(g)
	5.8×10^3	0.18	2π	1.80311	3.4577	1.355* / 0.2418**	Fig. 2(h)
Fig. 1(e)	2.83×10^5	0.25	2.5π	1.01078	3.587	9.6078	Fig. 2(i)
	5.86×10^3	0.20	1.0π	1.88854	3.4539	0	Fig. 2(j)
Fig. 1(f)	1.79×10^5	0.25	2.5π	1.00075	3.592	9.7684	Fig. 2(k)
	3.6×10^3	0.20	2.5π	1.93784	3.4517	0	Fig. 2(l)

Table 1. Higher and lower Q-factors of each type of microring and the corresponding parameters. *The propagation constant difference between the curved waveguides ($\Delta\beta_c$). **The propagation constant difference between the straight waveguides ($\Delta\beta_s$).

and the propagation constant of curved waveguide can be changed by adjusting the curved waveguide width. In Table 1, we list the higher and lower Q-factors for each resonator in Figs. 1 and the corresponding parameters. The larger $\Delta\beta$ between the bus waveguide and ring waveguide can be observed to be one of factors to obtain high Q-factor microing resonator. The results also show that the pulley-type microing [Fig. 1(a)] and the racetrack microing with one bus waveguide [Fig. 1(e)] can provide a higher Q-factor after adjusting the bus waveguide width.

The bending loss of the microring resonators. The electric fields of the microrings listed in Table 1 are shown in Figs. 2. The results show that the electric field in the bus waveguide of the higher Q-factor microrings [Fig. 2 (a),(c),(e),(g),(i),(k)] is weaker than that in the lower Q-factor microrings [Fig. 2 (b),(d),(f),(h),(j),(l)], respectively. According to the statements mentioned above, $\Delta\beta$ at the coupling region in the high Q-factor microing is larger than that in the low Q-factor microing. For high Q-factor microing, the propagating light stored in the ring is difficult to couple back to the bus waveguide. Additionally, the pulley-type microing resonator in Fig. 2 (a) can provide the highest Q-factor of 7×10^5 due to the lower bending loss. The long interaction length of coupling region (concentrically curved waveguides) in the pulley-type microing can provide the lower bending loss than that of the other structures except the pulley-type racetrack microing [Fig. 1(d)].

The pulley-type racetrack microing as shown in Fig. 1(d) with the longest coupling region and large propagation constant difference between the curved waveguides, $\Delta\beta_c$, cannot obtain the higher Q-factor. It is due to the radius of the curved waveguide of the racetrack microing is much smaller than that of the circular microrings, which results in the larger bending loss from the curved bus waveguide.

In order to study the relation between the bending loss and the microing resonator wrapped by the curved waveguide, we calculate the bending loss of single curved waveguide and two concentrically curved waveguides. The single ring waveguide with the central radius, R_c, defined as $(R_0 + R_1)/2 = 4.43\,\mu m$ is schematically shown in Fig. 3(a),(b) illustrates the two concentric ring waveguides. The gap between two ring waveguides is $0.15\,\mu m$. The inner and outer waveguide widths are $0.2\,\mu m$ and $0.23\,\mu m$, respectively. We launch an impulse light into the ring and adopt the exponential decay fitting for the power detected in the ring to obtain the bending loss per propagation distance of ring waveguide by the method published in Ref. 7. Fig. 3(c) shows the bending loss per propagation distance of the single ring waveguide and the two concentric ring waveguides. We can observe that the bending loss of the two concentric ring waveguides is lower than that of the single ring waveguide, since the outer waveguide of the concentric ring waveguides can collect the light of the radiation loss of the inner waveguide and then couple the light back to the inner waveguide. Therefore, the bending loss of the ring can be reduced by wrapping curved bus waveguide.

For the microrings with the identical circumference, the central radius of the curved waveguide of the racetrack microing is smaller than that of the other circular microrings. Therefore, the total bending loss of racetrack microing resonator should be larger than the other type of microing resonator.
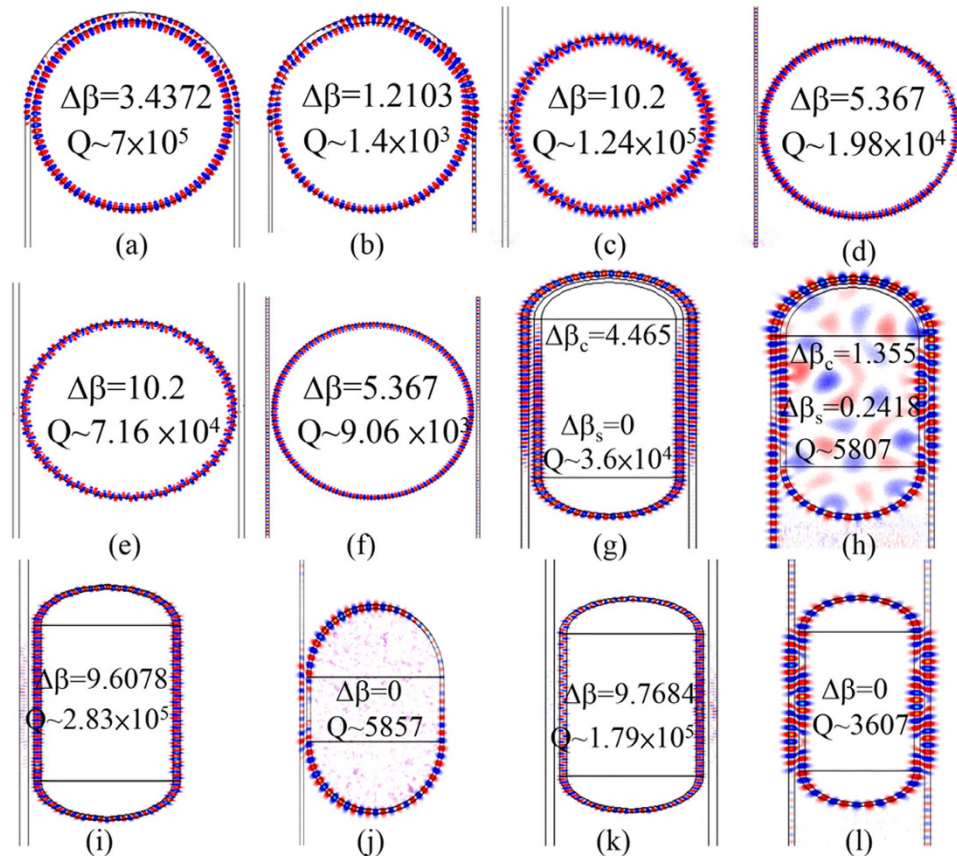
Figure 2. Normalized circulating field in the various microring resonators. For the identical type of microring resonator, the larger $\Delta\beta$ between bus waveguide and ring waveguide is helpful to obtain higher Q-factor. The corresponding resonance wavelengths and the widths of bus waveguide are listed in Table 1.

[The total bending loss (dB) of the microrings is defined as bending loss (dB/cm) × length of curved waveguide (cm). In our study, the bending loss (dB/cm) is obtained from Fig. 3(c).] The total bending loss of the microring with the single and two bus waveguides is identical to be 7.3×10^{-3} dB. The total bending loss of the pulley-type microring is 5×10^{-3} dB. In Fig. 3(c), we also illustrate the bending loss per propagation distance of the curved waveguide in the racetrack microring for different L. The total bending loss of the racetrack microring with L of 0.5π, π, 1.5π, 2π and 2.5π can be obtained to be 1.93×10^{-2} dB, 2.93×10^{-2} dB, 2.75×10^{-2} dB, 2.4×10^{-2} dB and 2.18×10^{-2} dB, respectively. The total bending loss of the pulley-type racetrack microring with L of 0.5π, π, 1.5π, 2π and 2.5π can be obtained to be 1.24×10^{-2} dB, 1.87×10^{-2} dB, 1.79×10^{-2} dB, 1.57×10^{-2} dB and 1.43×10^{-2} dB, respectively. The results show the pulley-type microring can provide lower bending loss than other types of microring.

The loss from output port. In order to investigate the power loss from Port B of the higher and lower Q-factor structures , we arrange thirty detectors at Port B as shown in Fig. 1(a),(d),(e). The distance between the detectors is around 80 nm. As the figures illustrated, the detector A is set to measure the power stored in the ring. The normalized power loss from Port B as shown in Fig. 4, which is defined as the power detected by the thirty detectors divided by the power detected by the detector A. The red line shows the normalized power losses for the pulley-type microring with d_3 of 0.23 μm ($Q = 7 \times 10^5$). The blue line shows the normalized power losses for the racetrack microring as shown in Fig. 1(e) with d_3 and L of 0.25 μm and 2.5π μm, respectively ($Q = 2.83 \times 10^5$). The decreasing of power as shown in Fig. 4 indicates that the circulating light in the bus waveguide at the output port is coupled to the ring waveguide. The output power measured at Detector 30 is almost the same to be around -40 dB, which indicates the fact that the critical coupling of the two structures is tuned to be almost identical. However, the Q-factor of the racetrack microring is lower than that of pulley-type microring with d_3 of 0.23 μm, since the smaller bending radius of the curved waveguide in the racetrack microring provides the higher bending loss than that of the pulley-type microring.

From the result in Fig. 3(c), we can conclude that the bending loss of pulley-type racetrack microring is lower than that of the racetrack microring. However, the Q-factor of the pulley-type racetrack microring is lower than that of racetrack microring. The green line in Fig. 4 shows the normalized power losses for the pulley-type racetrack microring with d_3 and L to be 0.2 μm and 2.5π μm, respectively
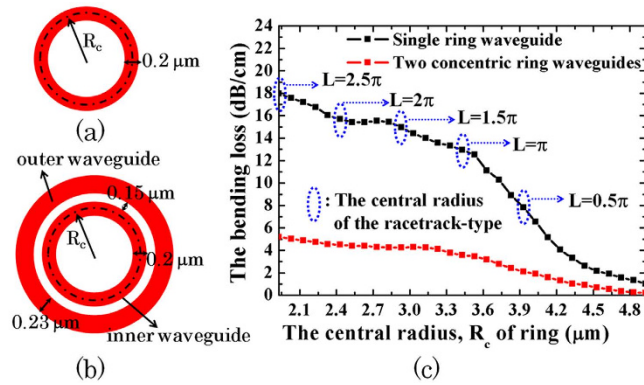
Figure 3. Bending loss. (**a**) and (**b**) show the schematic drawing of single ring waveguide and two concentric ring waveguides, respectively. (**c**) Bending loss per propagation distance of single ring waveguide and two concentric ring waveguides for different R_c are represented as the black line and red line, respectively.
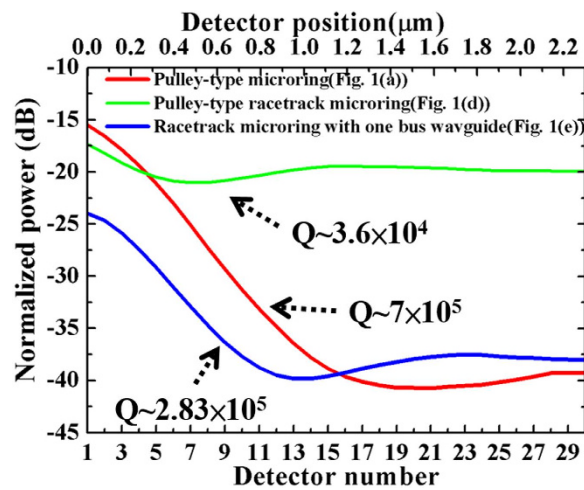

Figure 4. Power loss from output ports. The red, blue and green lines present the normalized power detected at Port B of the pulley-type microring resonator, the pulley-type racetrack microring resonator and the racetrack microring, respectively.

($Q = 3.6 \times 10^4$). We can observe that the measured power changes slightly from Detector 1 to Detector 30. The result indicates that the energy of the resonator losses from the output port. In this case, the critical coupling may not be as good as that in Fig. 2(a),(i) because the larger energy loss at the output port. From another viewpoint, among all structures that we analyze in this work, only the coupling region of the pulley-type racetrack microring consists of the straight waveguides and the curved waveguides. In this structure, the device parameters include the ring waveguide width, bus waveguide width, and radius of the ring and the gap width. The change of the parameters will individually change the coupling coefficient of the straight waveguides but also that of the curved waveguides. Therefore, the critical coupling of the pulley-type racetrack microring might be very difficult to be optimized.

In this work, we propose the guidelines to design the high-Q microring. Firstly, by wrapping the curved waveguide around the microring to form the pulley coupler, the bending loss can be effectively decreased. The longer interaction length of coupling region such as the concentrically curved waveguides is helpful to decrease the radiation loss and improve the Q-factor of the resonator. Secondly, the large difference of propagation constant, $\Delta\beta$, between the microring and the bus waveguide can maintain better the propagating light in the mcroring. Thirdly, the critical coupling can be rapidly optimized by adjusting the bus waveguide width to increase the Q-factor. The reasons mentioned above and the obtained results by comparing the performance of the different type ring resonators show that the pulley-type microring may provide higher Q-factor.

Method

Since the 3D-FDTD method is very time-consuming, in this work, we adopt the 2D FDTD method to investigate the in-plane energy decay in the microring[1,24].

Q-factor.

The Q-factor is calculated by monitoring the energy decay constant in the microring and exponential decay fitting. For the microring with the resonant wavelength at λ, the Q-factor is defined as

$$Q = \frac{2\pi\nu}{\alpha} \tag{1}$$

where ν and α are the frequency of light and the decay constant of stored energy, respectively.

The conformal transformation[15,22,23] method and Helmholtz equation.

The conformal transformation is the transformation preserved the local angle in the complex plane, w-plane. The analytic function in w-plane $w = f(z)$ cannot be conformal as the derivative of $f(z) = 0$ or ∞. In the conformal mapping, the analytic function $w = f(z)$ where $w = u + iv$ and $z = x + iy$ is employed to transform the structure of device from the original coordinate, z-plane, to a new coordinate, w-plane.

The conformal transformation method is suitably adopted to analyze the curved waveguide. The conformal transformation can transform the complex structure of curved waveguide to the simple structure of straight waveguide in such a way that

$$u = R_c \ln\left(\frac{R_c}{x}\right) \text{ and } v = R_c\theta \tag{2}$$

where u and v is the new coordinate after the transformation. R_c is the central radius of curved waveguide. x and y are respectively the coordinate and the angle before the transformation.

To obtain the propagation constant of curved waveguide, the wave equation is solved after the conformal transformation. Before the conformal transformation, the two dimensional scalar wave equation can be represented as

$$\left[\nabla^2_{x,y} + k^2(x, y)\right]\Phi(x, y) = 0 \tag{3}$$

The solution of equation (3) in new coordinate u, v can be defined by original coordinate x, y with the relation

$$w = u + iv = f(z) = f(x + iy) \tag{4}$$

where f is the analytic function. The Cauchy-Riemann equation and Laplace's equation are expressed as equation (5) and equation (6), respectively.

$$\frac{\partial x}{\partial v} = -\frac{\partial y}{\partial u} \,\&\, \frac{\partial x}{\partial u} = \frac{\partial y}{\partial v} \tag{5}$$

$$\frac{\partial^2 u}{\partial x^2} + \frac{\partial^2 u}{\partial y^2} = 0 \,\&\, \frac{\partial^2 v}{\partial x^2} + \frac{\partial^2 v}{\partial y^2} = 0 \tag{6a}$$

$$\frac{\partial^2 x}{\partial u^2} + \frac{\partial^2 x}{\partial v^2} = 0 \,\&\, \frac{\partial^2 x}{\partial u^2} + \frac{\partial^2 y}{\partial v^2} = 0 \tag{6b}$$

Expending the term of $\nabla^2_{x,\,y}$ in equation (3) by using equation (5) and equation (6a), the scalar wave equation can be rewritten as

$$\left[\nabla^2_{u,v} + \left|\frac{dz}{dw}\right|^2 k^2(u, v)\right]\Phi(u, v) = 0 \tag{7}$$

where

$$|dz/dw|^2 = \left[(\partial u/\partial x)^2 + (\partial v/\partial x)^2\right]^{-1}$$

By using the conformal transformation, w in equation (4) can be defined as

$$w = R_c \times \ln(z/R_c) \tag{8}$$

for which

$$\left|\frac{dz}{dw}\right| = \exp(u/R_c) \tag{9}$$

After the conformal transformation, the curved waveguide can be regarded as the straight waveguide. By separating the wave function $\Phi(u, v)$ into two functions:

$$\Phi(u, \quad v) = \varphi(u) \cdot \psi(v)$$

Equation (7) can be rewritten as the one-dimensional Helmholtz equation as

$$\left[\frac{\partial^2}{\partial u^2} + k_0^2 N^2(u)\right]\varphi(u) = \beta^2 \varphi(u) \tag{10}$$

where β is the propagation constant defined as $k_0 n_{eff}$. The effective index is n_{eff}. The $\phi(u)$ is the electric field distribution in w-plane. $N(u)$ defined as $n \cdot \exp(u/R_c)$ is the refractive index distribution in w-plane. After the conformal transformation, the step profile of refractive index can be transformed to the exponential profile of refractive index. By solving equation (10) as the eigen-problem, the effective indices (eigenvalues) and the corresponding electric fields (eigenvectors) can be obtained.

The bending loss.   The propagation loss of curved waveguide can be expressed as

$$\alpha = \frac{-2 \ln(\tau)}{L} \tag{11}$$

where τ is the attenuation of the circulating light per around trip. L is the length of the microring.

References

1. Little, B. E., Chu, S. T., Haus, H. A., Foresi, J. & Laine, J.-P. Microring Resonator Channel Dropping Filters. *J. Lightwave Technol.* **15,** 998–1005 (1997).
2. Matsko, A. B., Savchenkov, A. A., Ilchenko, V. S. & Maleki, L. Optical gyroscope with whispering gallery mode optical cavities. *Opt. Comm.* **233,** 107–112 (2004).
3. Scheuer, J & Yariv, A. Sagnac effect in coupled resonator slow light waveguide structures. *Phys. Rev. Lett.* **96,** 053901 (2006).
4. Almeida, V. R. *et al.* All-optical switching on a silicon chip. *Opt. Lett.* **29,** 2867–2869 (2004).
5. Scheuer, J., Paloczi, G. T., Poon, J. K. S. & Yariv, A. Coupled Resonator Optical Waveguides: Towards Slowing and Storing of Light. *Opt. Photon. News* **16,** 36–40 (2005).
6. Scheuer, J. Slow propagation of externally injected light pulses in coupled semiconductor laser array. *Europhysics. Lett.* **77,** 44004 (2007).
7. Niehusmann, J. *et al.* Ultrahigh-quality-factor silicon-on-insulator microring resonator. *Opt. Lett.* **29,** 2861–2863 (2004).
8. Goykhman, I., Desiatov, B. & Levy, U. Ultrathin silicon nitride microring resonator for biophotonic applications at 970 nm wavelength. *Appl. Phys. Lett.* **97,** 081108 (2010).
9. Forst, M. *et al.* High-speed all-optical switching in ion-implanted silicon-on-insulator microring resonators. *Opt. Lett.* **32,** 2046–2048 (2007).
10. Menon, V. M., Tong, W. & Forrest, S. R. Control of Quality Factor and Critical Coupling in Microring Resonators Through Integration of a Semiconductor Optical Amplifier. *IEEE Photon. Technol. Lett.* **16,** 1343–1345 (2004).
11. Poon, J. K. S., Scheuer, J., Xu, Y. & Yariv, A. Designing coupled-resonator optical waveguide delay lines. *J. Opt. Soc. Am. B* **21,** 1665–1673 (2004).
12. Hu, J. *et al.* Planar waveguide-coupled, high-index-contrast, high-Q resonators in chalcogenide glass for sensing. *Opt. Lett.* **33,** 2500–2502 (2008).
13. Hosseini, E. S., Yegnanarayanan, S., Atabaki, A. H., Soltani, M. & Adibi, A. Systematic design and fabrication of high-Q single-mode pulley-coupled planar silicon nitride microdisk resonators at visible wavelengths. *Opt. Express* **18,** 2127–2136 (2010).
14. Bi, L., Hu, J., Kimerling, L. & Ross, C. A. Fabrication and characterization of As₂S₃/Y₃Fe₅O₁₂ and Y₃Fe₅O₁₂/SOI strip-loaded waveguides for integrated optical isolator applications. *Proc. Of SPIE.* **7604,** 760406 (2010).
15. Cai, D. P., Chen, C. C., Lee, C. C. & Wang, T. D. Study of Coupling Length of Concentrically Curved Waveguides. *IEEE Photon. J.* **4,** 80–85 (2012).
16. Pandraud, G., Balbas, E. M., Yang, C. K. & French, P. J. Experimental Characterization of Roughness Induced Scattering Losses in PECVD SiC Waveguides. *J. Lightwave Technol.* **29,** 744–749 (2011).
17. Su, B., Wang, C., Kan, Q. & Chen, H. Compact Silicon-on-Insulator Dual-Microring Resonator Optimized for Sensing. *J. Lightwave Technol.* **29,** 1535–1541 (2011).
18. Vorckel, A., Monster, M., Henschel, W., Bolivar, P. H. & Kurz, H. Asymmetrically coupled silicon-on-insulator microring resonators for compact add-drop multiplexers. *IEEE Photon. Technol. Lett.* **15,** 921–923 (2003).
19. Stokes, L. F., Chodorow, M. & Shaw, H. J. All-single-mode fiber resonator. *Opt. Lett.* **7,** 288–290 (1982).
20. Yariv, A. Universal relations for coupling of optical power between microresonators and dielectric waveguide. *Electron. Lett.* **36,** 321–322 (2000).
21. M. N. Polyanskiy, RefractiveIndex INFO., (2008) Date of access: 30/05/2013 (Available at http://refractiveindex.info)
22. Heiblum, M. & Harris, J. H. Analysis of curved optical waveguides by conformal transformation. *IEEE J. Quantum Electron.* **QE-11,** 75–83 (1975).
23. Berglund, W. & Gopinath, A. WKB analysis of bend losses in optical waveguides. *J. Lightwave Technol.* **18,** 1161–1166 (2000).
24. Chu, S. T. & Chaudhuri, S. K. A finite-difference time-domain method for the design and analysis of guided-wave optical structure. *J. Lightwave Technol.* **7,** 2033–2038 (1989).

Author Contributions

D.P.C., J.H.L., C.C.C., C.C.L., C.E.L. and T.J.Y. designed and analyzed data. D.P.C. and J.H.L. executed the simulations. D.P.C., C.C.C., C.C.L., C.E.L. and T.J.Y. wrote the manuscript text. All authors reviewed the manuscript.

Additional Information

Competing financial interests: The authors declare no competing financial interests.

How to cite this article: Cai, D.-P. *et al.* High Q-factor microring resonator wrapped by the curved waveguide. *Sci. Rep.* **5**, 10078; doi: 10.1038/srep10078 (2015).